Modeling and Numerical Simulation of Material Science, 2026, 16(3), 45-59
https://www.scirp.org/journal/mnsms
ISSN Online: 2164-5353
ISSN Print: 2164-5345

Numerical Performance Analysis of an Environment-Friendly High-Efficiency Copper-Based Perovskite Solar Cell Using SCAPS-1D Software

Sunirmal Kumar Biswas[1*], Shahariar Hasan Rumel[1], Hossain Mohammad Maruf Rahman Shuvo[1], Md Shorif[1], Jalal Uddin Mohammad Akbar[1], Md. Mostak Ahmed[1], Palash Chandra Karmaker[2]

[1]Department of Electrical and Electronic Engineering, Prime University, Dhaka, Bangladesh
[2]Department of Physics, Gono Bishwabidyalay, Savar, Dhaka, Bangladesh
Email: *sunirmalkumar@primeuniversity.edu.bd, rjrumel394@gmail.com, marufrahmanshuvo@gmail.com, uddinmdshorif72@gmail.com, mdakbar2351@gmail.com, mostakahmedpu@gmail.com, pckarmakerpu@gmail.com

How to cite this paper: Biswas, S.K., Rumel, S.H., Shuvo, H.M.M.R., Shorif, M., Akbar, J.U.M., Ahmed, M.M. and Karmaker, P.C. (2026) Numerical Performance Analysis of an Environment-Friendly High-Efficiency Copper-Based Perovskite Solar Cell Using SCAPS-1D Software. *Modeling and Numerical Simulation of Material Science*, **16**, 45-59.
https://doi.org/10.4236/mnsms.2026.163003

Received: April 28, 2026
Accepted: July 5, 2026
Published: July 8, 2026

Abstract

In this research, we investigated the potential of the hybrid organic-inorganic material $(CH_3NH_3)_2CuCl_4$ as an absorber in perovskite solar cells (PSCs). Perovskite solar cells are becoming more popular as a potential boost to the efficiency of traditional photovoltaic cells. The advantages of this cell over commercial silicon or other organic and inorganic solar cells are its high efficiency and eco-friendliness. In this study, we used the SCAPS-1D software to improve device performance parameters, employing ZnSe as the electron transport layer and $SrCu_2O_2$, a promising hole-transport material identified in $(CH_3NH_3)_2CuCl_4$ - based perovskite solar cells (PSCs). To further enhance device performance, we have analyzed the effects of absorber and buffer layer thickness, acceptor density, absorber defect density, and interfacial defect densities at the ETL/Absorber and Absorber/HTL interfaces. In addition, we analyzed the effects of operating temperature, series resistance, and shunt resistance on the quantum efficiency, back contact materials, current density-voltage, and overall optimum device performance. Gold is utilized for the back contact. The efficient perovskite solar cell achieved an exceptionally high efficiency of 28.5% with a 0.05 μm buffer layer and a 0.6 μm absorber layer. The proposed solar cell structure may enable high-performance perovskite solar cells.

Keywords

Solar Energy, Perovskite Solar Cell, Thin Film, SCAPS-1D, $SrCu_2O_2$

1. Introduction

Scientists have been studying alternative energies for decades, since fossil fuels are dirty and finite. We will inevitably look for other energy sources. Fossil fuel sources are becoming harder to find. Consequently, the focus of scientific inquiry has shifted to sustainable energy, with solar energy remaining the primary source. Directly converting solar radiation into electrical power is a form of harnessing solar energy [1] [2]. The development of third-generation thin-film photovoltaic (PV) technology has led to perovskite solar cells (PSCs). Perovskite solar cells have mechanical, optical, and physical characteristics that make them appropriate for photovoltaic systems. Scholars have examined some of these attributes through density functional theory and first-principles computation [3]-[6].

Double- or stacked-perovskite materials are the most promising approach for creating lead-free PSCs. This technique substitutes one monovalent M^{+} cation and one divalent M^{2+} cation for the traditional two divalent Pb cations inside the perovskite structure. Consequently, these double perovskites have the following chemical structure: $A_2M^{+}M^{2+}X_6$, where A can be $CH(NH_2)$ or CH_3NH^{3+} [7]. With its creative structural design, ecologically friendly PSCs could be produced without sacrificing functionality, providing a more sustainable and clean method of solar energy harvesting. We used ZnSe as a buffer layer because it is low-cost and highly transparent, which improves overall device efficiency [8]. With a broad 2.7 eV bandgap, ZnSe is a significant technical optoelectronic semiconductor. ZnSe is a suitable replacement for solar photovoltaic cells. It is regarded as a crucial technical material because of its potential uses in various optical and electrical devices, as well as in buffer and window materials for thin-film heterojunction solar cells [9]. This study used $SrCu_2O_2$ as an HTL layer because oxides are more chemically stable and less moisture-sensitive than many organic or halide materials. Using $SrCu_2O_2$ may improve device stability, particularly in operational/ambient exposure. For SCAPS modeling, this supports selecting buffer parameters with less drift (stable defect densities and lifetimes) and exploring stability under temperature variation [10]. It has been discovered that inorganic p-type transparent conductive oxides (TCOs), such as $SrCu_2O_2$, are excellent hole conductors for solar cells with suitable valence and conduction band positions [11]-[14].

The proposed perovskite solar cell used $(CH_3NH_3)_2CuCl_4$ as an absorber layer for Lead-free, lower toxicity, replacing Pb with Cu makes $(CH_3NH_3)_2CuCl_4$ an attractive, environmentally friendlier absorber for lead-free perovskite device concepts, which is an important design consideration in simulation studies to explore non-toxic alternatives [15]. And also used ITO as an ETL layer because it has a realistic bandgap of ITO (~3.5 - 4.0 eV), so it doesn't absorb visible light significantly [16]. In this simulation, we introduce an ITO/ZnSe/$(CH_3NH_3)_2CuCl_4$ /$SrCu_2O_2$/Au perovskite solar cell. During this simulation, a total efficiency of 28.5% was gained. This proposed perovskite solar cell can be used for its high-efficiency application.

2. Numerical Simulation and Parameters of Materials

The computational model's framework provides an understanding of the fundamentals of solar cells and the key parameters influencing their performance. Crucial one-dimensional semiconductor equations can be solved directly through the SCAPS-1D software [17]. The continuity equations for electrons and holes are as follows:

$$-\left(\frac{1}{q}\right)\frac{d_{jn}}{dx}-Un+G=\frac{d_n}{dt} \tag{1}$$

$$-\left(\frac{1}{q}\right)\frac{d_{jp}}{dx}-Up+G=\frac{d_p}{dt} \tag{2}$$

where Jn and Jp are electron and hole current densities, and G is the generation rate. The Poisson equation is

$$\frac{d^2}{dx^2}\psi(x)=\frac{e}{\varepsilon_o\cdot\varepsilon_r}\left[\rho(x)-n(x)+N_D-N_A+\rho_P-\rho_n\right] \tag{3}$$

The electrostatic potential is represented by ψ, the electrical charge is represented by e, the relative and vacuum permittivity by ε_r and ε_0, the concentrations of holes and electrons are represented by p and n, respectively, the charge impurities of the acceptor and donor types are represented by N_A and N_D, and the distributions of holes and electrons are represented by ρ_P and ρ_n [18]. The literature and the user manual for SCAPS, a very potent program for solar cell performance, provide descriptions of the program and the algorithms it employs [19]-[22]. For this $(CH_3NH_3)_2CuCl_4$-based Perovskite solar cell, **Figure 1** displays the schematic diagram. **Figure 2** presents the energy band alignment for various materials utilized in the proposed perovskite solar cell. **Table 1** shows the simulation of the material parameters used in the proposed solar cell.

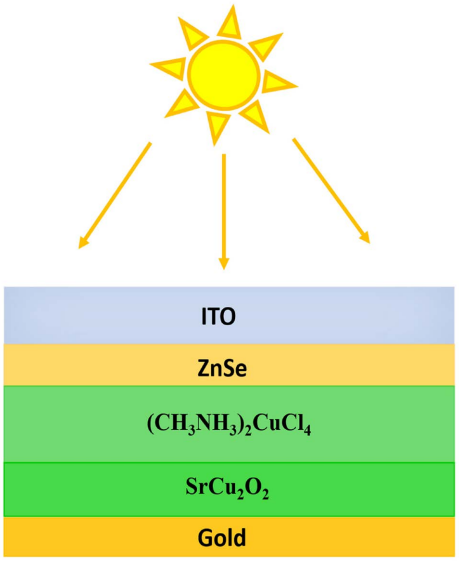

Figure 1. Schematic diagram of a proposed perovskite solar cell.

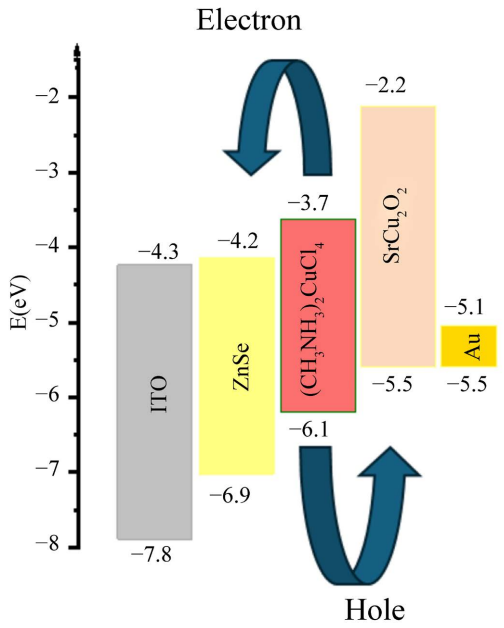

Figure 2. Energy band alignment for various materials utilized in the proposed perovskite solar cell.

Table 1. For the simulation, the material parameters were used in the proposed solar cell.

Material Parameter	ITO [41]	ZnSe [9]	$(CH_3NH_3)_2CuCl_4$ [15]	$SrCu_2O_2$ [10]
Thickness (μm)	0.1	0.05	0.6	0.2
Band Gap (eV)	3.5	2.9	1.2	3.3
Electron Affinity (eV)	4	4.1	4.17	2.2
Dielectric Permittivity	9	10	10	9.7
CB effective Density (cm^{-3})	2.2×10^{18}	1.5×10^{18}	2×10^{18}	2×10^{20}
VB effective Density (cm^{-3})	1.8×10^{19}	1.8×10^{19}	1.8×10^{18}	2×10^{21}
Electron Thermal Velocity (cm/s)	10^7	10^7	10^7	10^7
Hole Thermal Velocity (cm/s)	10^7	10^7	10^7	10^7
Electron Mobility (cm^2/V-s)	20	50	3	0.1
Hole Mobility (cm^2/V-s)	100	20	1	0.46
Donor Density N_D (cm^{-3})	1×10^{21}	1×10^{18}	0	0
Acceptor Density N_A (cm^{-3})	0	0	1×10^{18}	1×10^{17}
Total Defect Density (cm^{-3})	1×10^{14}	1×10^{13}	1×10^{15}	1×10^{15}

3. Results and Discussions

3.1. Effect of Absorber Layer Thickness

The thickness of the absorber layer is a significant factor in establishing the device's specifications. The absorber layer thickness on the perovskite solar cell (PSC)

is depicted in Figure 3. The thickness of the absorber layer varies from 0.2 μm to 2 μm. Figure 3 shows that all solar cell performance parameters, such as Open Circuit Voltage (Voc), Short Circuit Current (Isc), Fill Factor (FF), and efficiency, have improved. Efficiency increases from 22.8% to 28.5%, Isc from 24.62 mA/cm^2 to 34.76 mA/cm^2, and FF from 85.05% to 85.5%. From 0.97 V to 0.94 V, Voc falls. Due to enhanced light absorption, the Power Conversion Efficiency (PCE) increases from 22.8% to 28.5%. By increasing the thickness of the absorber layer, the absorber layer improves light absorption and carrier generation, thereby increasing the short-circuit current density [23].

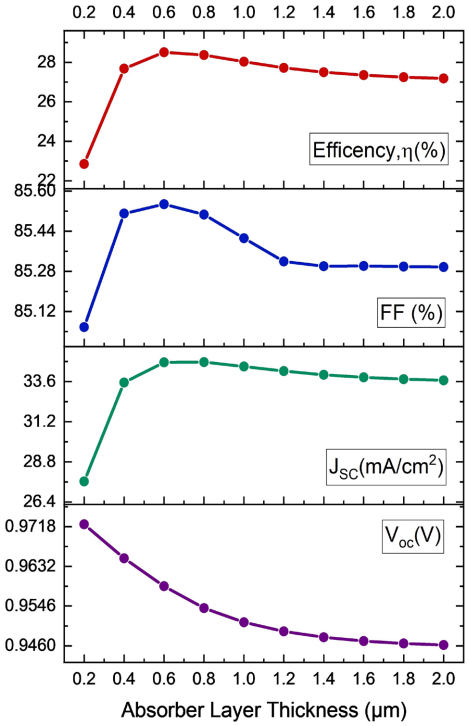

Figure 3. Effect of absorber layer thickness on the solar cell parameters.

3.2. Effect of Buffer Layer Thickness

Figure 4 shows the effect of the Electron Transport Layer (ETL) layer on the perovskite solar cell. ETL thickness varies from 0.01 μm to 0.05 μm. It shows that all the PV parameters are slightly increased, but the values are almost constant.

The change is negligible; in this simulation, 0.05 μm was the optimized ETL thickness, with an Open Circuit Voltage (Voc) of 0.95 V, a Short Circuit Current Density (Jsc) of 34.75 mA/cm^2, a Fill Factor (FF) of 85.54%, and an efficiency of 28.5%. This suggests that there is not much impact of ETL thickness on the perovskite solar cells (PSC's) electrical properties [24].

3.3. Effect of Series & Shunt Resistance

Figure 5(a)-(b) illustrates how series and shunt resistance affect the solar cell.

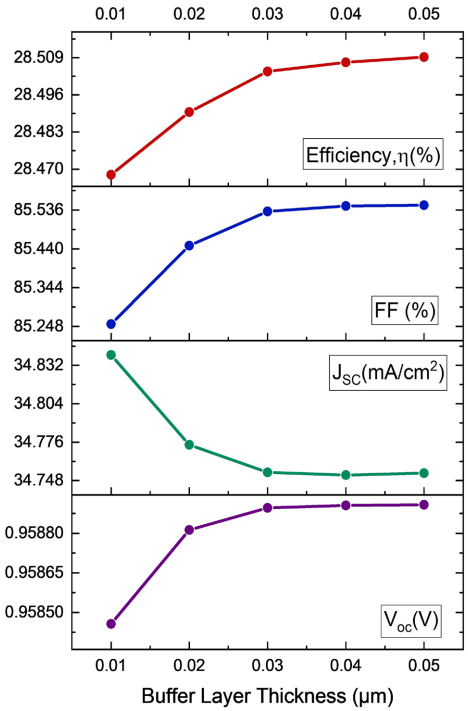

Figure 4. Effect of buffer layer thickness on the solar cell parameters.

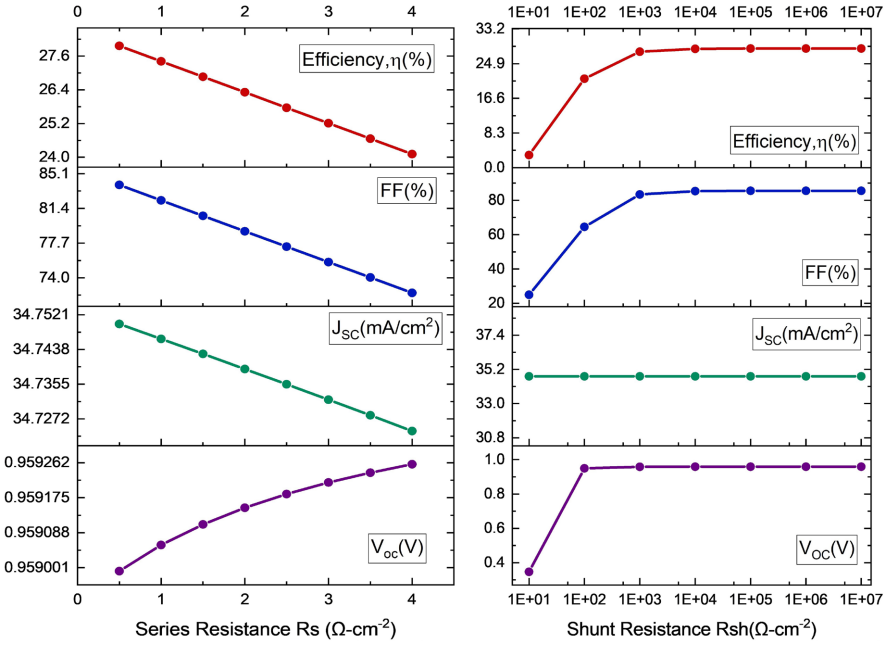

Figure 5. (a): Effect of series resistance on the solar cell parameters. (b): Effect of shunt resistance on the solar cell parameters.

The series resistance is changed in **Figure 5(a)** from 0.5 Ω cm^{-2} to 4 Ω cm^{-2}. It has been noted that, apart from Jsc, all solar cell properties decrease as series resistance rises. Fill Factor (FF) diminishes as the series resistance increases. At higher re-

sistance values, the short-circuit current decreases [25]. Here, equations 4 and 5 illustrate how series resistance affects the performance metrics.

$$I_{SG} = I_o\left(e\frac{Vocq}{nkT} - 1\right) \tag{4}$$

$$I_{SG} = I_l - I_o\left(e\frac{Vocq}{nkT} - 1\right) - \frac{V_{OC} + I_{SCRS}}{rsh} \tag{5}$$

where R_{sh} represents shunt resistance, and I_L represents light-induced current. The math above shows that when R_S rises, the Short Circuit Current (I_{SC}) decreases [26] [27]. **Figure 5(b)** demonstrates the effect of shunt resistance on the proposed perovskite solar cell (PSC). The shunt resistance is varied from 1E1 Ωcm^{-2} to 1E7 Ωcm^{-2}. As seen, all the parameters improve with variation. It's noticeable that there isn't much effect on the short circuit current. Shunt resistance losses predominantly originate from defect-state recombination; hence, higher shunt resistance indicates fewer defect states [28].

3.4. Effect of Temperature

Figure 6 shows the effect of temperature on the solar cell, with temperature ranging from 275 K to 400 K. All the metrics, except short-circuit current, decrease gradually. This may result from a decline in efficiency brought on by the defect density in the layers rising with temperature. Temperature-related increases in deformation stress may lead to a decrease in the device's efficiency [29]. Here, Open Circuit Voltage (Voc) decreases from 0.987 V to 0.83 V, Fill Factor (FF) 86.5% to 80.2%, and Power

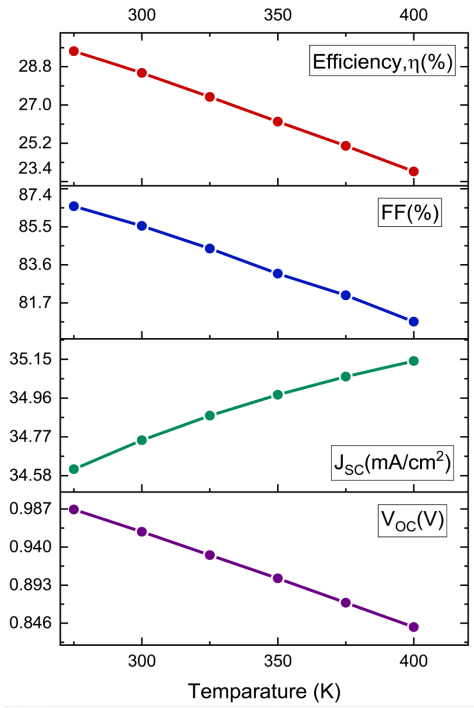

Figure 6. Effect of temperature on the solar cell parameters.

Conversion Efficiency (PCE) 29.3% to 23%. Because temperature alters the diffusion length, which raises the series resistance, the device's FF and efficiency are reduced [30]. For this device simulation, an optimized temperature of 300 K was used.

3.5. Effect of Defect Density

The impact of absorber-layer defect density on the solar cell is shown in **Figure 7**. In this case, the defect varies between 1E12 cm^{-3} and 1E18 cm^{-3}. This variation affects every parameter in this case. Power Conversion Efficiency (PCE) decreases from 36% to 5%. Short Circuit Current (Isc) ranges from 35.6 mA/cm^2 to 11 mA/cm^2, Fill Factor decreases (FF) from 87.6% to 65%, and Open Circuit Voltage (Voc) from 1.1 V to 0.62 V. An increase in defect density reduces carrier lifetimes because more recombination and traps are present, making paths more accessible. This lowers effective carrier mobility [31]. Defects must occur in all materials to achieve high efficiency at low defect concentrations [32]. For this reason, we selected an absorber layer defect density of 1E15 cm^{-3}.

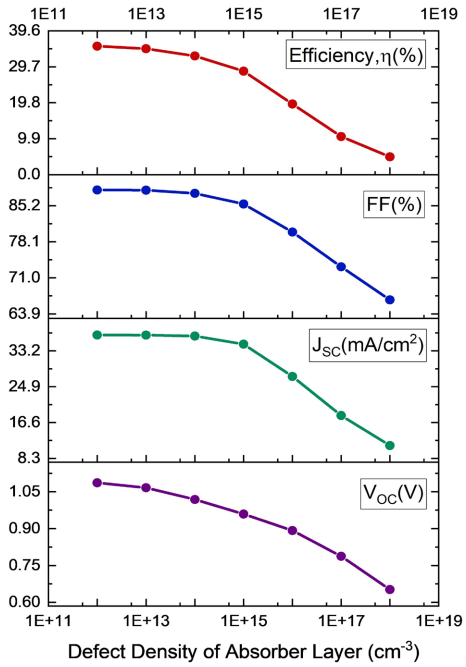

Figure 7. Effect of defect density of absorber layer on the solar cell parameters.

3.6. Quantum Efficiency

Figure 8 shows the quantum efficiency vs wavelength characteristics curve. It shows the highest absorption in the visible wavelength range. There is a noticeable decline in quantum efficiency in the infrared. In this case, the absorber layer ranges from 0.2 to 2 μm. An optimal thickness of 0.6 μm was obtained for this simulation. **Figure 8** shows that as the absorber layer thickness increases, the quantum efficiency rises at longer wavelengths. This is because there aren't enough photons in the absorber layer to generate sufficient electron-hole pairs [33].

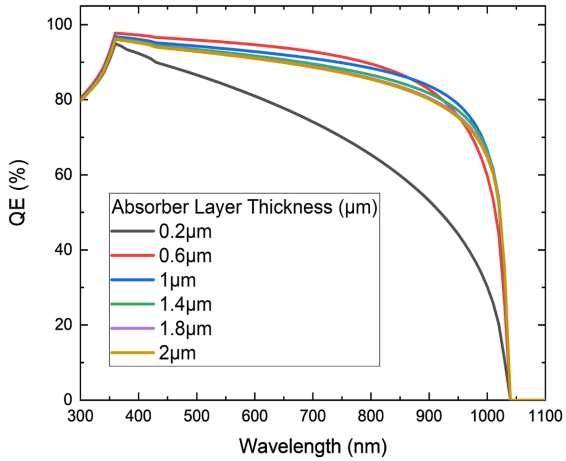

Figure 8. Quantum efficiency characteristics of the PSC solar cell.

3.7. Current Density-Voltage Characteristics

Figure 9 displays the solar cell's J-V properties. In this simulation, the thickness of the absorber layer is adjusted from 0.2 μm to 2 μm.

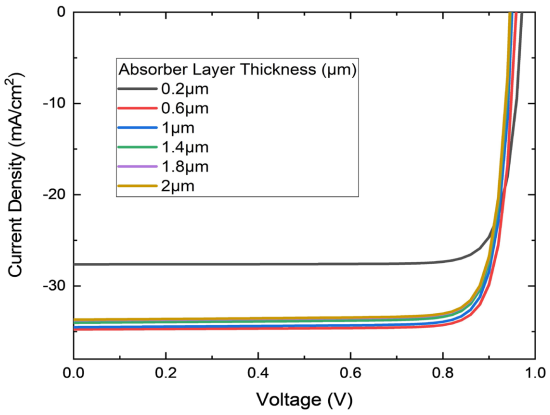

Figure 9. Current-voltage characteristics of the PSC solar cell.

Here, 0.6 μm was the ideal thickness for the absorber layer, resulting in an Open Circuit Voltage (Voc) of 0.95 V, Short Circuit Current (Isc) of 34.75 mA/cm^2, Fill Factor (FF) of 85.54%, and efficiency of 28.5%. When the absorber is thickened, the electron-hole pair is added, which raises the voltage and current [34].

3.8. Interface Defect

Table 2 shows the interface defect density for the device.

Table 2. The interface defect density for the device.

Interface Defect Parameters	ET L/Absorber	HTL/Absorber
Defect Type	Neutral	Neutral
Capture Cross Section Electrons (cm^2)	1E−19	1E−19
Capture Cross Section Holes (cm^2)	1E−19	1E−19

Continued

Energetic Distribution	Single	Single
Reference for Defect Energy Level Et	Above the Highest eV	Above the Highest eV
Energy with Respect to Reference (eV)	0.6	0.6
Total Density (Integrated Over All Energies) (cm^{-2})	1E10–1E14	1E10–1E14

3.9. Effect of ETL/Absorber and Absorber/HTL Interface Defect Density

The impact of interface defect density on the suggested perovskite solar cell is depicted in Figure 10. This simulation changes the Electron Transport Layer (ETL)/Absorber layer and the Absorber/Hole Transport Layer (HTL) interface from 1E10 cm^{-3} to 1E14 cm^{-3}.

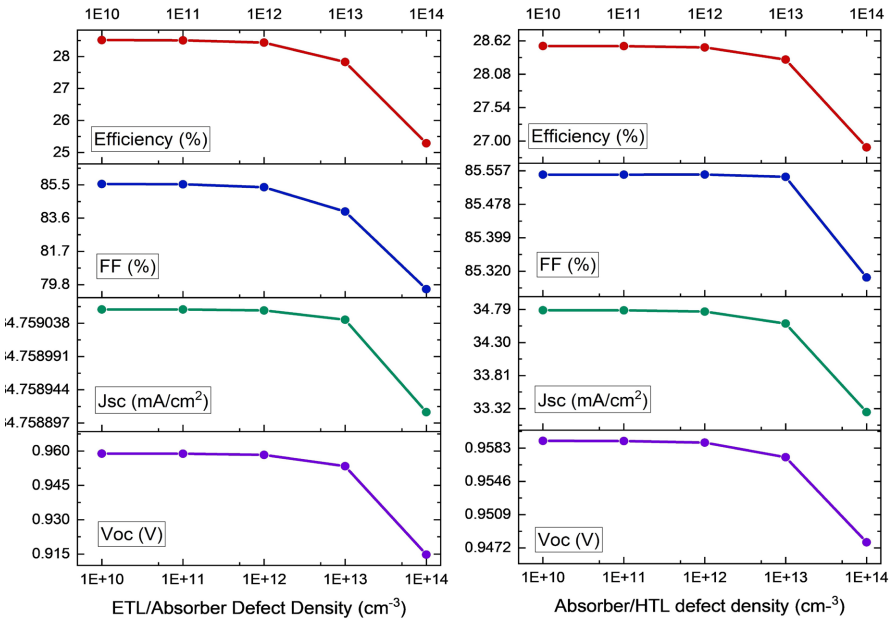

Figure 10. (a): Effect of ETL/Absorber on the solar cell parameters. (b): Absorber/HTL defect density on the solar cell parameters.

Through simulation, it is found that interface fault densities significantly impact all the parameters. Low photocurrent generation and overall efficiency are caused by high defect density because it creates mid-gap trap states that serve as recombination without radiation focal points, restricting diffusion length and carrier lifetime [35]. Figure 10(b) shows the Absorber/Hole Transport Layer (HTL) defect density on the proposed perovskite solar cell. High interface defect density causes efficiency to drop quickly. Defects cause recombination centers for charging carriers, which lowers efficiency and current density [36]. Because of this, an interface defect density of less than 1E11 cm^{-3} [37] and a thickness of 0.6 μm are required for the maximum efficiency.

3.10. Effect of Back Contact Material

Table 3 presents the Metal work function for different materials.

Table 3. Metal work functions for different materials.

Back Contact Metal	Ag	Fe	Au	Cu	Cu Doped C
Work Function	4.7	4.8	5.3	4.6	5.0

The metal's quantity of energy is known as the work function or the number of photons necessary to eliminate a single electron from its surface [38]. Improved solar cell efficiencies have been associated with higher work function values [39] [40]. Au and Pt are expensive metals frequently employed as back contacts in solar cells. In this work, simulations were conducted to identify an appropriate, commercially available metal for the back contact of the proposed device configuration. Figure 11 shows the impact of various materials used for the back contact on the PCE. The maximum efficiency achieved in this instance was 28.5%.

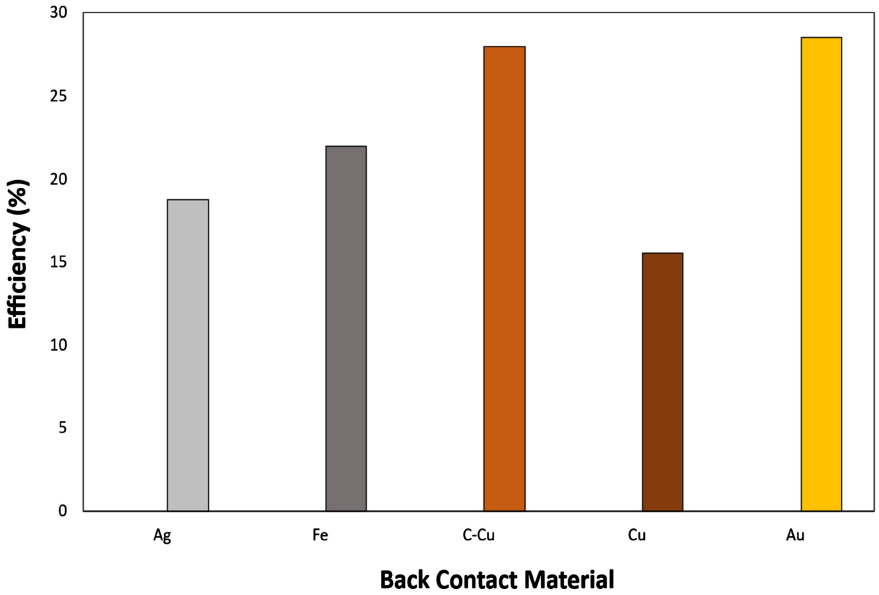

Figure 11. Different back contact materials' effects on solar cells.

4. Conclusion

A novel copper-based perovskite solar cell was studied using SCAPS 1D simulation software in this research. This study analyzes the effects of absorber layer thickness, buffer layer thickness, absorber layer defect density, series resistance, and shunt resistance to determine the optimized values. Furthermore, the quantum efficiency and current-voltage characteristics were investigated for the proposed perovskite solar cell. After simulation, the optimum values of the absorber layer thickness (0.6 μm) and the total defect density (N_t = 1E15 cm^{-3}) were obtained. It's observed that at 300K, the device performs at its highest level. After

simulation, Voc 0.95 V, Jsc 34.75 mA/cm^2, FF 85.54%, and efficiency 28.5% were obtained as the optimized values. Overall, this proposed perovskite solar cell is observed as a high-efficiency, green, and stable heterojunction cell.

Acknowledgements

The authors would like to thank Dr. Marc Burgelman and his colleagues at the Department of Electronics and Information Systems (ELIS), University of Gent, Belgium, for providing the SCAPS simulation package.

Data Availability Statement

The data that support the findings of this study are available from the corresponding author upon reasonable request.

Conflicts of Interest

The authors declare no conflicts of interest regarding the publication of this paper.

References

[1] Şen, Z. (2004) Solar Energy in Progress and Future Research Trends. *Progress in Energy and Combustion Science*, **30**, 367-416. https://doi.org/10.1016/j.pecs.2004.02.004

[2] Al-Hattab, M., Moudou, L., Khenfouch, M., Bajjou, O., Chrafih, Y. and Rahmani, K. (2021) Numerical Simulation of a New Heterostructure CIGS/GaSe Solar Cell System Using SCAPS-1D Software. *Solar Energy*, **227**, 13-22. https://doi.org/10.1016/j.solener.2021.08.084

[3] Litimein, F., Khenata, R., Bouhemadou, A., Al-Douri, Y. and Omran, S.B. (2012) First-Principle Calculations to Investigate the Elastic and Thermodynamic Properties of *R*BRh_3(R=Sc, Y and La) Perovskite Compounds. *Molecular Physics*, **110**, 121-128. https://doi.org/10.1080/00268976.2011.635607

[4] Moulai, N., Ameri, M., Azaz, Y., *et al.* (2015) Predictive Study of Structural, Electronic, Magnetic and Thermodynamic Properties of $XFeO_3$ (X=Ag, Zr and Ru) Multiferroic Materials in Cubic Perovskite Structure: First-Principles Calculations. *Materials Science-Poland*, **33**, 402-413, https://doi.org/10.1515/msp-2015-0058

[5] Reshak, A.H., Abu-Jafar, M.S. and Al-Douri, Y. (2016) Two Symmetric N-Type Interfaces $SrTiO_3$/$LaAlO_3$ in Perovskite: Electronic Properties from Density Functional Theory. *Journal of Applied Physics*, **119**, Article 245303. https://doi.org/10.1063/1.4954293

[6] Bidai, K., Ameri, M., Amel, S., Ameri, I., Al-Douri, Y., Varshney, D., *et al.* (2017) First-Principles Calculations of Pressure and Temperature Dependence of Thermodynamic Properties of Anti-Perovskite BiNBa3 Compound. *Chinese Journal of Physics*, **55**, 2144-2155. https://doi.org/10.1016/j.cjph.2017.03.023

[7] Pal, J., Manna, S., Mondal, A., Das, S., Adarsh, K.V. and Nag, A. (2017) Colloidal Synthesis and Photophysics of $M_3Sb_2I_9$ (m=Cs and Rb) Nanocrystals: Lead-Free Perovskites. *Angewandte Chemie International Edition*, **56**, 14187-14191. https://doi.org/10.1002/anie.201709040

[8] Buba, A. (2016) Optoelectronic Properties of Zinc Selenide (ZnSe) Thin Films Deposited Using Chemical Bath Deposition (CBD) Technique. *British Journal of Applied*

Science & Technology, **14**, 1-7. https://doi.org/10.9734/bjast/2016/23622

[9] Abdalameer, N.K., Mazhir, S.N. and Aadim, K.A. (2020) The Effect of ZnSe Core/Shell on the Properties of the Window Layer of the Solar Cell and Its Applications in Solar Energy. *Energy Reports*, **6**, 447-458. https://doi.org/10.1016/j.egyr.2020.09.023

[10] Noman, M., Shahzaib, M., Jan, S.T., Shah, S.N. and Khan, A.D. (2023) 26.48% Efficient and Stable $FAPbI_3$ Perovskite Solar Cells Employing $SrCu_2O_2$ as Hole Transport Layer. *RSC Advances*, **13**, 1892-1905. https://doi.org/10.1039/d2ra06535e

[11] Nie, X., Wei, S.H. and Zhang, S.B. (2002) First-Principles Study of Transparent p-Type Conductive $SrCu_2O_2$ and Related Compounds. *Physical Review B*, **65**, Article 075111. https://doi.org/10.1103/physrevb.65.075111

[12] Shasti, M. and Mortezaali, A. (2019) Numerical Study of Cu_2O, $SrCu_2O_2$, and $CuAlO_2$ as Hole-Transport Materials for Application in Perovskite Solar Cells. *Physica Status Solidi A*, **216**, Article 1900337. https://doi.org/10.1002/pssa.201900337

[13] Bandara, J. and Yasomanee, J.P. (2006) P-Type Oxide Semiconductors as Hole Collectors in Dye-Sensitized Solid-State Solar Cells. *Semiconductor Science and Technology*, **22**, 20-24. https://doi.org/10.1088/0268-1242/22/2/004

[14] Zhao, Y., Dong, W., Fang, X., Zhou, Y., Meng, G., Tao, R., *et al.* (2012) P-Type Ca Doped $SrCu_2O_2$ Thin Film: Synthesis, Optical Property and Photovoltaic Application. *Journal of Alloys and Compounds*, **513**, 50-54. https://doi.org/10.1016/j.jallcom.2011.09.067

[15] Elseman, A.M., Shalan, A.E., Sajid, S., Rashad, M.M., Hassan, A.M. and Li, M. (2018) Copper-Substituted Lead Perovskite Materials Constructed with Different Halides for Working $(CH_3NH_3)_2CuX_4$-Based Perovskite Solar Cells from Experimental and Theoretical View. *ACS Applied Materials & Interfaces*, **10**, 11699-11707. https://doi.org/10.1021/acsami.8b00495

[16] Liu, X., Wang, L. and Tong, Y. (2020) Optoelectronic Properties of Ultrathin Indium Tin Oxide Films: A First-Principle Study. *Crystals*, **11**, Article 30. https://doi.org/10.3390/cryst11010030

[17] Burgelman, M., Nollet, P. and Degrave, S. (2000) Modelling Polycrystalline Semiconductor Solar Cells. *Thin Solid Films*, **361**, 527-532. https://doi.org/10.1016/s0040-6090(99)00825-1

[18] Biswas, S.K., Mim, M.K. and Ahmed, M.M. (2023) Design and Simulation of an Environment-Friendly ZrS_2/$CuInS_2$ Thin Film Solar Cell Using SCAPS 1D Software. *Advances in Materials Science and Engineering*, **2023**, 1-10. https://doi.org/10.1155/2023/8845555

[19] Kumar, A. and Sharma, P. (2023) Transfer Matrix Method-Based Efficiency Enhancement of Lead-Free $Cs_3Sb_2Br_9$ Perovskite Solar Cell. *Solar Energy*, **259**, 63-71. https://doi.org/10.1016/j.solener.2023.05.014

[20] Prasanna, J.L., Goel, E. and Kumar, A. (2023) Numerical Investigation of MAPbI3 Perovskite Solar Cells for Performance Limiting Parameters. *Optical and Quantum Electronics*, **55**, Article No. 610. https://doi.org/10.1007/s11082-023-04876-9

[21] Burgelman, M., Decock, K., Niemegeers, A., *et al.* (2016) SCAPS Manual. https://scaps.elis.ugent.be/SCAPS%20manual%20most%20recent.pdf

[22] Dastan, D., Mohammed, M.K.A., Al-Mousoi, A.K., Kumar, A., Salih, S.Q., JosephNg, P.S., *et al.* (2023) Insights into the Photovoltaic Properties of Indium Sulfide as an Electron Transport Material in Perovskite Solar Cells. *Scientific Reports*, **13**, Article No. 9076. https://doi.org/10.1038/s41598-023-36427-3

[23] Bakirci, K. (2012) The Effect of Absorber Layer Thickness on the Performance of Solar

Cells. *Renewable Energy*, **37**, 67-70.

[24] Sarker, K., Sumon, M.S., Orthe, M.F., Biswas, S.K. and Ahmed, M.M. (2023) Numerical Simulation of High Efficiency Environment Friendly $CuBi_2O_4$-Based Thin-Film Solar Cell Using SCAPS-1D. *International Journal of Photoenergy*, **2023**, 1-11. https://doi.org/10.1155/2023/7208502

[25] Chakraborty, K., Choudhury, M.G. and Paul, S. (2019) Numerical Study of Cs_2TiX_6 (X=Br^-, I^-, F^- and Cl^-) Based Perovskite Solar Cell Using SCAPS-1D Device Simulation. *Solar Energy*, **194**, 886-892. https://doi.org/10.1016/j.solener.2019.11.005

[26] Heriche, H., Rouabah, Z. and Bouarissa, N. (2017) New Ultra Thin CIGS Structure Solar Cells Using SCAPS Simulation Program. *International Journal of Hydrogen Energy*, **42**, 9524-9532. https://doi.org/10.1016/j.ijhydene.2017.02.099

[27] Jeon, N.J., Noh, J.H., Yang, W.S., *et al.* (2015) Compositional Engineering of Perovskite Materials for High-Performance Solar Cells. *Nature*, **517**, 476-480.

[28] Naureen, S., Lohia, P., Dwivedi, D. and Ameen, S. (2022) A Comparative Study of Quantum Dot Solar Cell with Two Different ETLs of WS2 and IGZO Using SCAPS-1D Simulator. *Solar*, **2**, 341-353. https://doi.org/10.3390/solar2030020

[29] Srivastava, P., Rai, S., Lohia, P., Dwivedi, D.K., Qasem, H., *et al.* (2022) Theoretical Study of Perovskite Solar Cell for Enhancement of Device Performance Using SCAPS-1D. *Physica Scripta*, **97**, Article 125004. https://doi.org/10.1088/1402-4896/ac9dc5

[30] Biswas, S.K., Sumon, M.S., Sarker, K., Orthe, M.F. and Ahmed, M.M. (2023) A Numerical Approach to Analysis of an Environment-Friendly Sn-Based Perovskite Solar Cell with SnO_2 Buffer Layer Using SCAPS-1D. *Advances in Materials Science and Engineering*, **2023**, 1-10. https://doi.org/10.1155/2023/4154962

[31] Mishra, S., Bhargava, K. and Deb, D. (2019) Numerical Simulation of Potential Induced Degradation (PID) in Different Thin-Film Solar Cells Using SCAPS-1D. *Solar Energy*, **188**, 353-360. https://doi.org/10.1016/j.solener.2019.05.077

[32] Karthick, S., Velumani, S. and Bouclé, J. (2020) Experimental and SCAPS Simulated Formamidinium Perovskite Solar Cells: A Comparison of Device Performance. *Solar Energy*, **205**, 349-357. https://doi.org/10.1016/j.solener.2020.05.041

[33] Sunny, A., Rahman, S., Khatun, M.M. and Ahmed, S.R.A. (2021) Numerical Study of High Performance HTL-Free $CH_3NH_3SNi_3$-Based Perovskite Solar Cell by SCAPS-1D. *AIP Advances*, **11**, Article 065102. https://doi.org/10.1063/5.0049646

[34] Li, H., Ali, W., Wang, Z., Mideksa, M.F., Wang, F., Wang, X., *et al.* (2019) Enhancing Hot-Electron Generation and Transfer from Metal to Semiconductor in a Plasmonic Absorber. *Nano Energy*, **63**, Article 103873. https://doi.org/10.1016/j.nanoen.2019.103873

[35] Mim, M.K. and Biswas, S.K. (2025) Performance Analysis of Sr_3SbI_3-Based Perovskite Solar Cell Using SCAPS-1D Software. *Advances in Materials Science and Engineering*, **2025**, Article 7134012. https://doi.org/10.1155/amse/7134012

[36] Khatoon, S., Chakraborty, V., Yadav, S.K., Diwakar, S., Singh, J. and Singh, R.B. (2023) Simulation Study of CsPbIxBr1-X and MAPbI3 Heterojunction Solar Cell Using SCAPS-1D. *Solar Energy*, **254**, 137-157. https://doi.org/10.1016/j.solener.2023.02.059

[37] Chowdhury, M.S., Shahahmadi, S.A., Chelvanathan, P., Tiong, S.K., Amin, N., Techato, K., *et al.* (2020) Effect of Deep-Level Defect Density of the Absorber Layer and N/I Interface in Perovskite Solar Cells by SCAPS-1D. *Results in Physics*, **16**, Article 102839. https://doi.org/10.1016/j.rinp.2019.102839

[38] Anwar, F., Afrin, S., Satter, S., *et al.* (2017) Simulation and Performance Study of Nanowire CdS/CdTe Solar Cell. *International Journal of Renewable Energy Research*, **7**, 885-893.

[39] Derry, G.N., Kern, M.E. and Worth, E.H. (2015) Recommended Values of Clean Metal Surface Work Functions. *Journal of Vacuum Science & Technology A*: *Vacuum*, *Surfaces*, *and Films*, **33**, Article 060801. https://doi.org/10.1116/1.4934685

[40] Thahab, S.M., Abu Hassan, H. and Hassan, Z. (2006) Effects of Metal Work Function and Operating Temperatures on the Electrical Properties of Contacts to N-Type Gan. 2006 *IEEE International Conference on Semiconductor Electronics*, Kuala Lumpur, 29 November-1 December 2006, 816-819.

[41] Ganem, H.T. and Saleh, A.N. (2021) Enhancement of the Efficiency of the CzTs/-CdS/ZnO/ITO Solar Cell by Back Reflection and Buffer Layers Using SCAPS-1D. *Iraqi Journal of Science*, **62**, 1144-1157. https://doi.org/10.24996/ijs.2021.62.4.11